Synthesis of N doped titania nanotube arrays photoanode using urea as nitrogen precursor for photoelectrocatalytic application

IOP Conf. Series: Materials Science and Engineering **509** (2019) 012144 doi:10.1088/1757-899X/509/1/012144

Synthesis of N doped titania nanotube arrays photoanode using urea as nitrogen precursor for photoelectrocatalytic application

Tiur Elysabeth[1], Slamet[1,*], Athiek Sri Redjeki

[1] Department of Chemical Engineering, Faculty of Engineering, Universitas Indonesia, Depok 16424, Indonesia

* Corresponding author: slamet@che.ui.ac.id; slamet.dtk.ui@gmail.com

Abstract. Addition of urea as nitrogen precursor during synthesis of TiO_2 nanotube arrays photocatalyst has been investigated. This study aimed to increase the visible light photo response of TiO_2 by applying nitrogen doped titania nanotube arrays (N-TNTAs) for photoanode preparation in the photoelectrocatalytic process. Nitrogen doped titania nanotube arrays (N-TNTAs) was synthesized by a one-step electrochemical anodization method at 50 V for 2 hour, in the electrolyte solution containing water, ammonium fluoride, glycerol and specified amounts of urea as nitrogen precursor followed by annealing at 500°C for 3 h to induce crystallization. Amount of urea (0.1, 0.2 and 0.4 wt%) in electrolyte solution and annealing atmosphere (air and N_2) were varied to enhance visible light photo response. SEM analysis showed that TNTAs and N-TNTAs were successfully synthesized with diameters of 64–320 nm but the morphologies did not show a significant difference. The XRD results showed an identical pattern dominated by the anatase phase. The size of N-TNTAs crystallite is larger than the undoped TNTAs. UV-DRS analysis showed that N-TNTAs have smaller bandgap energy. The smallest bandgap energy was obtained 2.84 eV from N-TNTAs using 0.2% urea with N_2 gas annealing (N-TNTAs 0.2% U-N_2). Measurement of photocurrent density showed better activity under visible light with smaller bandgap energy.

Keywords: Titania nanotube, nitrogen precursor, nitrogen doping, photoelectrocatalytic

1. Introduction

In the photoelectrocatalytic process, photoanode material has an important role as a place for the hole and electron excitation process so that electrons can be channelled to the cathode and used for reduction process. In addition, photoanode is also the place where the oxidation process takes place. The use of TiO_2 as photoanode has several advantages, high chemical stability, non-toxic, high efficiency and relatively cheap price [1]. However, TiO_2 has the disadvantages, one of which is a wide band gap (3-3.2 eV) [2] so that it is only activated by UV light. The amount of UV light emitted by solar energy is only around 4-5%, much smaller than the amount of visible light which is around 45% [3]. Another problem is the high recombination hole and electron level [4]. The disadvantages make TiO_2 less suitable for use on an industrial scale.

There are several ways to overcome the disadvantages of TiO_2, one of which is modifying the properties of TiO_2. Modifications are made to enlarge the range of visible light absorption by decreasing bandgap energy. Many researchers have succeeded in reducing bandgap energy by non-metal doping such as boron, carbon, sulphur, fluorine, and nitrogen [5-10]. Asahi *et al.* [5] reported that increasing activity of TiO_2 under visible light can be achieved by adding nitrogen to the TiO_2 structure. According

to Hu *et al.* [11] hybridization of orbital O 2p and N 2p on the valence band or the mid-gap formation induced by ions causes a decrease in bandgap energy so that TiO_2 activity under visible light can increase. Nitrogen doping has also been shown to inhibit the transformation of anatase to rutile to increase crystallinity of anatase [9]. TiO_2 nanotubes with nitrogen doping can be synthesized with several methods including ion implantation, chemical deposition, ammonia gas annealing at high and low temperatures and anodizing titanium plates with electrolyte solutions containing nitrogen precursors [12].

In the present work, synthesis of nitrogen doped TiO_2 nanotubes will be carried out by one step anodization of titanium plate with glycerol as a electrolyte solution which containing urea as a nitrogen precursor and adding nitrogen gas flow during annealing process. The nitrogen doping effects on the morphology and structure of undoped TNTAs and N-TNTAs will be analysed by scanning electron microscopy–energy dispersive X-ray (SEM-EDX) and X-ray diffraction (XRD). Bandgap energy of undoped TNTAs and N-TNTAs will be observed by diffuse reflectance spectroscopy (DRS). Since the synthesized TiO_2 will be used as a photoanode in the photoelectrocatalytic process, so photoelectrochemical property of undoped TNTAs and N-TNTAs will be examined by anodic photocurrent response.

2. Experimental

2.1. Materials

Titanium foils with a thickness of 0.3 mm and purity of 99.6% was supplied by Baoji Jinsheng Metal Material Co. Ltd. HNO_3 (Merck, 65%) and HF (Merck, 40%) were used as chemical polished. Glycerol (Brataco),NH_4F (Merck, 98%) were used as electrolyte solution. Urea (Merck, P.A) was used as nitrogen precursor and N_2 was used as annealing gas.

2.2. Synthesis of nitrogen doped titania nanotube (N-TNTAs)

The Ti foil (3.0 cm x 2.0 cm) was mechanically polished with sand papers, then chemically polished in the mix solution of hydrofluoric acid, nitric acid and water (1:3:6) for 2 min. Synthesis of TNTAs was carried out by anodizing of Ti foil with 60 ml of electrolyte solution. Electrolyte solution contained glycerol, 0.5 wt% ammonium fluoride, 25 wt% water and varying content of urea (U) (0.1 wt%, 0.2 wt% and 0.4 wt%) were used as electrolyte solution. The anodization used two-electrode system, Ti foil as anode and Pt foil as cathode and was carried out at a potential of 50 V for 2 hours by using a DC power supply under magnetically stirring. After anodization process, samples were rinsed with distilled water and continued with thermal annealing process at a temperature of 500°C for 3 hours in furnace to crystallize them then naturally cooled to the ambient temperature. The thermal annealing process was held under air and N_2 gas.

2.3. Characterization of undoped and nitrogen doped titania nanotube

The morphological analysis of undoped and nitrogen doped titania nanotube were done by Scanning Electron Microscope, SEM (ZEISS) using accelerating voltage 20 kV. The samples composition was determined by Energy Dispersive X-ray analyser (EDX) which is attached to the SEM. The band-gap energy of the samples was observed by UV diffuse reflectance spectroscopy (UV-DRS) using Spectrophotometer Shimadzu UV 2450 type in wavelength range of 200-800 nm and calculated by Kubelka-Munk factor. The crystallography of N-TNTAs and undoped TNTAs were identified using Shimadzu X-ray Diffractometer (XRD) 7000 Maxima-X type with the scan rate at 2° min^{-1} over the scan range 10-80° and it was operated at 40 KV and 30 mA with the source of X-ray radiation was Cu Niα (λ=0.15406 nm). The size of crystallite was estimated from FWHM (full width at half maximum) by Scherrer equation.

2.4. Measurement of photocurrent density

The performance of electrode was tested in photoelectrochemical cell using a cylindrical vessel and three electrodes with TNTAs or N-TNTAs foil as a working electrode, a platinum foil as the counter electrode and Ag/AgCl as a reference electrode. The photoelectrochemical cell was equipped with 11 Watt visible lights (Krisbow) and 1 M KOH as electrolyte solutions. The measurement of photocurrent density was done with linear sweep voltammetry method and used a scanning potentiostate (eDAQ, version 9.1) to perform a potentiodynamic scan from-1.0 V to 1.0 V at a rate of 10mV S^{-1}.

3. Results and discussion

3.1. Morphology of TNTAs and N-TNTAs

SEM images of TNTAs and N-TNTAs are presented in Fig. 1. As seen in the picture that there was no significant change in the morphology of TNTAs before being doped or after being doped with nitrogen. The morphology of nanotubular structure was observed in all titania nanotube samples. This is predicted because the addition of urea is small amount. From the results of SEM, it was found that the average diameter of TNTAs, N-TNTAs 0.1%U-Air, N-TNTAs 0.2%U-Air, N-TNTAs 0.4%U-Air, N-TNTAs 0.1%U-N_2, N-TNTAs 0.2%U-N_2 and N-TNTAs 0.4%U-N_2 were 60-320 nm, 60-270, 60-190 nm, 60-316 nm, 60-250 nm, 60-317 nm and 60-198 nm. The difference in tube diameter is due to the forming of nanotubes during anodization process. Another study reported that TNTAs synthesized by the anodization process produced varying tube diameter ranges [13].

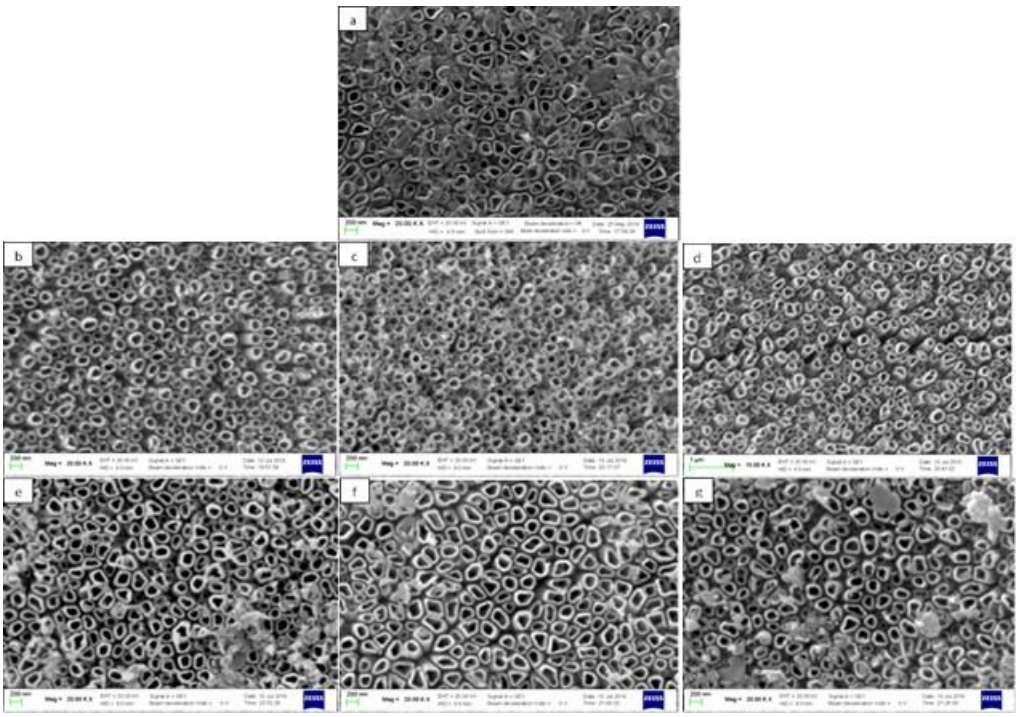

Figure 1. Top view image of SEM for (a) TNTAs, (b) N-TNTAs (0.1%U-Air), (c) N-TNTAs (0.2%U-Air), (d) N-TNTAs (0.4%U-Air), (e) N-TNTAs (0.1%U-N_2), (f) N-TNTAs (0.2%U-N_2) and (g) N-TNTAs (0.4%U-N_2).

EDX analysis was used to find out the elements contained on the surface of TNTAs. Fig. 2 and Table 1 showed that the main elements found in TNTAs are Ti and O. Other elements such as C and N are also detected. This is because these elements are absorbed during anodization on the surface of the nanotubes. The source of N comes from NH_4F [14] and in this study N also comes from urea [12]. However, elements detected by EDX cannot represent elements that enter the TNTAs matrix. So it

cannot be ascertained the number of N elements that replace or adsorb and are bound to O atoms from TNTAs. In this study, the results of EDX analysis showed the number of N elements found on the surface increased with increasing concentration of urea, although the increasing is not significant.

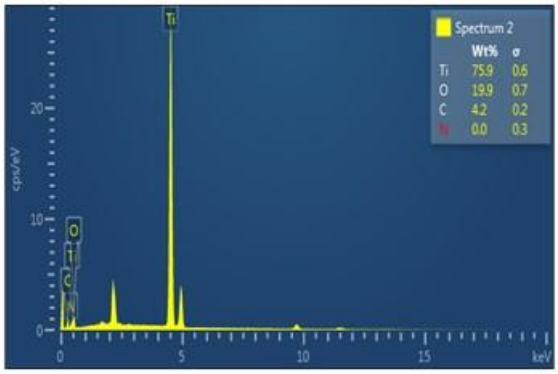

Figure 2. EDX analysis and nitrogen content of TNTAs and N-TNTAs.

Table 1. Nitrogen content of TNTAs and N-TNTAs.

Sample	N (% α)
TNTAs	0.43
N-TNTAs (0.1%U-Air)	0.29
N-TNTAs (0.2%U-Air)	0.52
N-TNTAs (0.4%U-Air)	0.56
N-TNTAs (0.1%U-N_2)	0.52
N-TNTAs (0.2%U-N_2)	0.51
N-TNTAs (0.4%U-N_2)	0.56

Fig. 3 showed the effect of adding urea in TNTAs to the structure and crystallite size of photocatalyst. The figure showed that the TNTAs and N-TNTAs crystal structure after 3 hours of annealing at 500°C has 100% anatase phase. The anatase phase can observed 2θ=25°, 48° and 53°. XRD results show identical patterns, this is due to the fact that the N elements that enter the TiO_2 matrix do not significantly affect the crystal structure of TiO_2 [15]. Because N atoms enter the TNTAs matrix, the diffraction peaks for N are undetectable because these atoms are dispersed evenly and only slightly in TNTAs [16]. In this study, the addition of urea increases the size of the crystallite. These crystallite sizes are larger than anatase crystallite of TiO_2 P25 (20 nm) [13]. Anatase crystallite size is calculated by the Debye-Scherrer equation [14]. The results of the calculation of the crystallite size are shown in Fig. 3 (insert).

The entry of the N dopant in the TNTAs matrix has also shifted a little diffraction angle in the larger direction (d spacing change). This phenomenon is caused by certain TNTAs matrices having changed with the existence of dopants [17]. Nitrogen doping also inhibited the transformation of anatase to rutile to increase crystallinity of anatase [9].

Fig. 4 showed the UV-DRS reflectance spectra of various photocatalysts and Fig. 5 showed the Tauc plot used to estimate the bandgap energy. UV-DRS Spectra was used to see the effect of adding urea on bandgap energy from photocatalyst. Kubelka-Munk function was applied to determine the band gap energy [13] as follow:

$$[F(R).h\upsilon]^{1/2} = K(h\upsilon - Eg) \quad (1)$$

Where $F(R)=(1-R)^2/2R$; R is reflectance, hυ is photon energy and K is the constant characteristic of TiO_2. For photocatalyst TiO_2, Tauc plot $\{F(R).h\upsilon]^{1/2}$ on hυ provides a linear line on optical light

absorption. By extrapolating the Tauc chart on a linear section and cutting on the x axis, the bandgap energy can be evaluated as shown in Fig. 5 (insert).

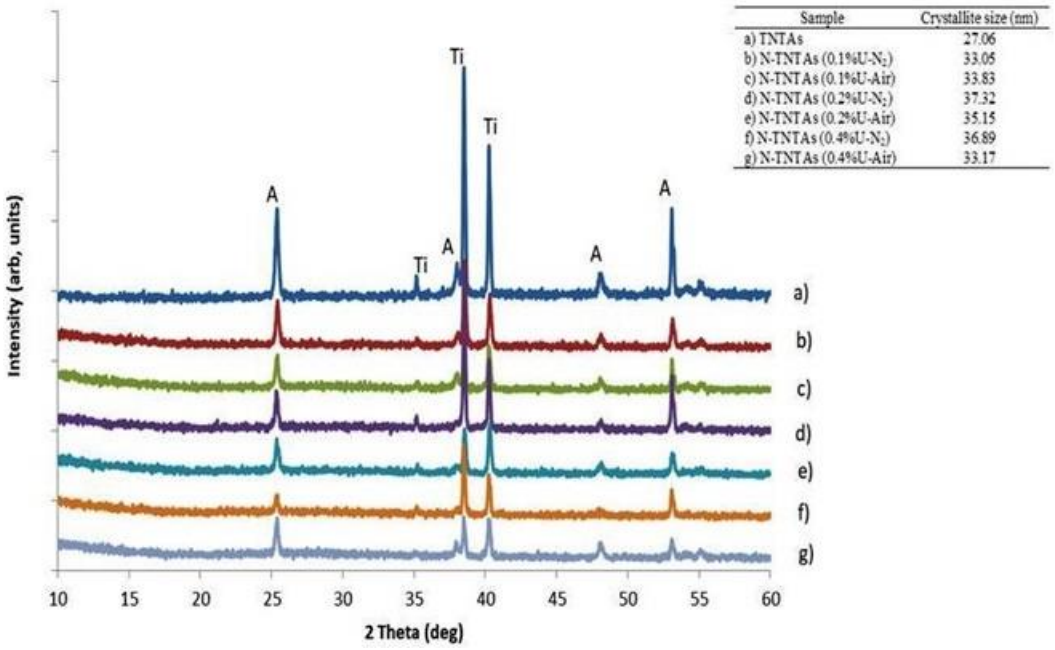

Figure 3. XRD patterns and crystallite size of the TNTAs and N-TNTAs.

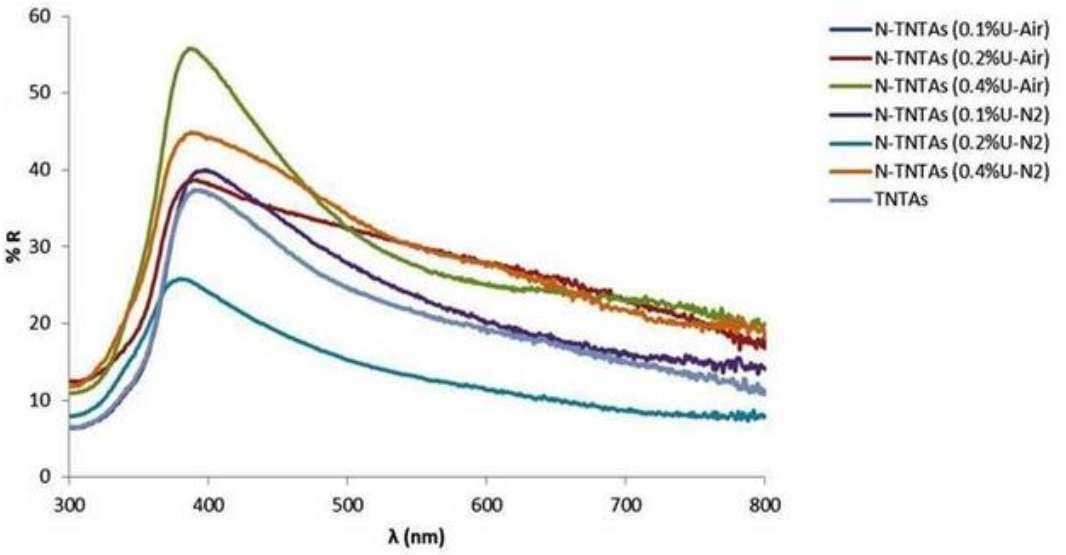

Figure 4. UV-DRS reflectance spectra of the TNTAs and N-TNTAs.

Fig. 5 showed that N doped photocatalyst has decreased energy bandgap. This is due to the entry of N atoms into the TNTAs matrix and form N-Ti-O bonds in the valence band so as to increase the energy level and decrease the band gap [9]. Annealing of photocatalyst with N_2 gas showed a greater decrease in bandgap energy. This is because annealing with N_2 gas can promote the oxidation of N elements in TNTAs and help incorporate these elements into the TNTAs structure. The results showed all photocatalyst in this research have a lower bandgap energy than TiO_2 P25 (3.28 eV) [13]. It might increase photo response to visible light so that the photocatalytic activity under visible light could be better.

The calculation results showed that N-TNTAs 0.2%U has smaller band gap energy than N-TNTAs 0.4%U. It is presumably because the higher the concentration of urea, the larger the size of the molecule so that the diffusion rate becomes lower. The low diffusion level causes the decreasing of N atoms number entering the TiO_2 matrix.

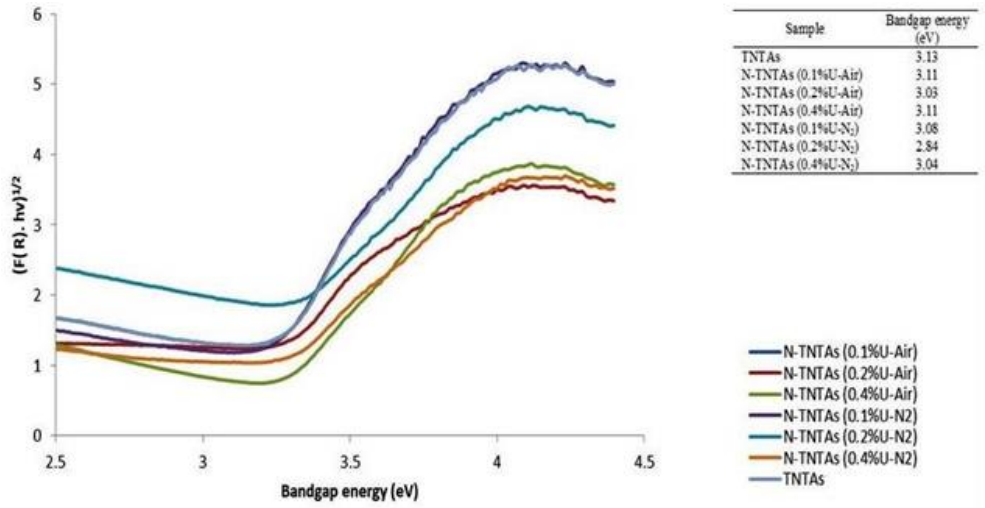

Sample	Bandgap energy (eV)
TNTAs	3.13
N-TNTAs (0.1%U-Air)	3.11
N-TNTAs (0.2%U-Air)	3.03
N-TNTAs (0.4%U-Air)	3.11
N-TNTAs (0.1%U-N_2)	3.08
N-TNTAs (0.2%U-N_2)	2.84
N-TNTAs (0.4%U-N_2)	3.04

Figure 5. Tauc plot from Kubelka-Munk function vs energy (eV) for TNTAs and N-TNTAs.

3.2. Photocurrent density of undoped and nitrogen dopes titania nanotube

Photocurrent density measurement was carried out to describe the number of electrons flowing from the anode to the cathode when the photocatalyst was illuminated by visible light. With the help of voltage, the electron will move to the inside of the photocatalyst and flow to the counter electrode, Pt, while the hole will move to the surface of the photocatalyst. The amount of current density represents the high activity of photocatalyst when exposed to visible light. The high excited electrons from the valence band to the conduction band and the low recombination of electron-holes will cause high electrons to move from the anode to the cathode [18].

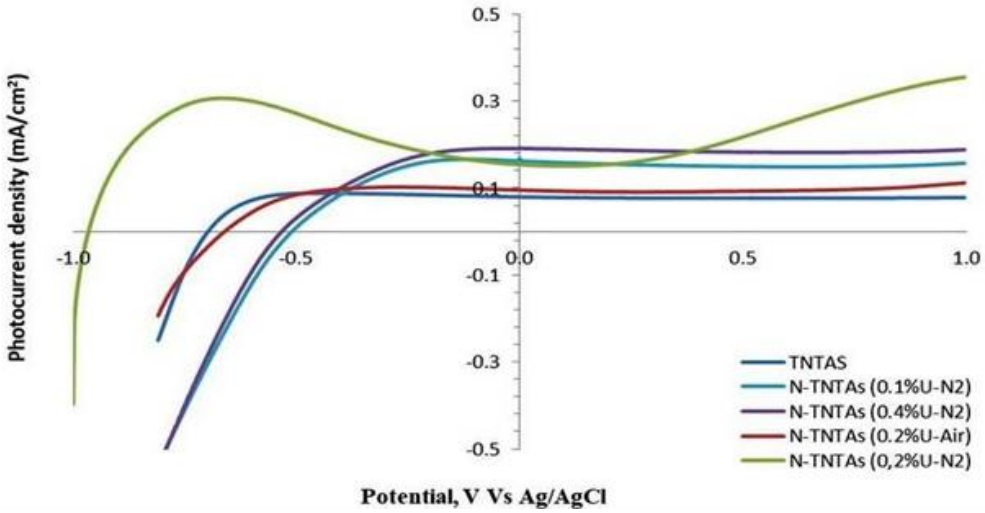

Figure 6. Photocurrent density of undoped and nitrogen doped titania nanotube in visible light illumination.

The relationship between photocurrent density and voltage with visible light can be seen in Fig. 6. In the figure it can be seen that N-TNTAs (0.2% U-N_2) provide a high response to visible light irradiation. This is proportional to the value of the bandgap energy. Theoretically, photocatalysts with low bandgap energy will have higher photocurrent density. In addition, the N doping increases oxygen vacancies and narrow band gap [5]. The high efficiency of photocurrent conversion could be contributed to enhance the optical absorption capability caused by the N-doping [19]. TiO_2 photocatalytic activity depends on the transfer rate of surface charge carriers from the bulk to the surface and rate of photogenerated electrons and holes recombination. This study showed the consistent results in the properties of TiO_2 in which N doped can reduce bandgap energy, improve the photoresponse to visible light and promote the electron-hole excitation by visible light [20].

4. Conclusion

The result of SEM showed that TNTAs and N-TNTAs were successfully synthesized with diameters of 64–320 nm. The morphology of nanotubular structure was observed in all samples. The doping N in TNTAs did not show significant changes in morphology. This is due to the small amount of urea added as nitrogen precursor. The results of EDX analysis showed an increase in N composition after adding urea. However, the amount of N detected cannot represent N entering the matrix and bounded to O. The pattern of the crystal structure also showed no significant difference, all of which have 100% anatase phase. Addition of urea caused the size of the crystal to be larger. The entry of the N in the TNTAs matrix has shifted a little diffraction angle in the larger direction. The results of the DRS analysis showed that bandgap energy has decreased after TiO_2 was doped N. The value of photocurrent density is higher with decreasing bandgap energy. High photocurrent density showed the better photocatalytic activity in visible light irradiation.

Acknowledgement

This work is supported by Hibah PITTA 2018 funded by DRPM Universitas Indonesia No.5000/UN2.R3.1/HKP.05.00/2018

References

[1] Wang X, Zhao H, Quan X, Zhao Y and Chen S 2009 Visible light photoelectrocatalysis with salicylic acid-modified TiO2 nanotube array electrode for p-nitrophenol degradation *J. Hazard. Mater.* **166** 1 547-52
[2] Lee K, Mazare A and Schmuki P 2014 One-dimensional titanium dioxide nanomaterials: nanotubes *Chem. Rev.* **114** 19 9385-454
[3] Kisch H, Sakthivel S, Janczarek M and Mitoraj D 2007 A low-band gap, nitrogen-modified titania visible-light photocatalyst *J. Phys. Chem. C.* **111** 30 11445-9
[4] Chen S, Chu W, Huang Y, Liu X and Tong D 2012 Preparation of porous nitrogen-doped titanium dioxide microspheres and a study of their photocatalytic, antibacterial and electrochemical activities *Mater. Res. Bull.* **47** 12 4514-21
[5] Asahi R, Morikawa T, Ohwaki T, Aoki K and Taga Y 2001 Visible-light photocatalysis in nitrogen-doped titanium oxides *Sci.* **293** 5528 269-71
[6] Yu J C, Yu J, Ho W, Jiang Z and Zhang L 2002 Effects of F-doping on the photocatalytic activity and microstructures of nanocrystalline TiO2 powders *Chem. Mater.* **14** 9 3808-16
[7] Ohno T, Mitsui T and Matsumura M 2003 Photocatalytic activity of S-doped TiO2 photocatalyst under visible light *Chem. Lett.* **32** 4 364-5
[8] Lee J-Y, Park J and Cho J-H 2005 Electronic properties of N-and C-doped Ti O 2 *Appl. Phys. Lett.* **87** 1 011904
[9] Cheng X, Yu X and Xing Z 2012 Characterization and mechanism analysis of N doped TiO2 with visible light response and its enhanced visible activity *Appl. Surf. Sci.* **258** 7 3244-8
[10] Chen D, Yang D, Wang Q and Jiang Z 2006 Effects of boron doping on photocatalytic activity and microstructure of titanium dioxide nanoparticles *Ind. Eng. Chem. Res.* **45** 12 4110-6

[11] Hu C-C, Hsu T-C and Lu S-Y 2013 Effect of nitrogen doping on the microstructure and visible light photocatalysis of titanate nanotubes by a facile cohydrothermal synthesis via urea treatment *Appl. Surf. Sci.* **280** 171-8
[12] Mazierski P, Nischk M, Gołkowska M, Lisowski W, Gazda M, Winiarski M J, Klimczuk T and Zaleska-Medynska A 2016 Photocatalytic activity of nitrogen doped TiO2 nanotubes prepared by anodic oxidation: The effect of applied voltage, anodization time and amount of nitrogen dopant *Appl. Catal. B.* **196** 77-88
[13] Gunlazuardi J and Dewi E L 2014 Effect of NaBF4 addition on the anodic synthesis of TiO2 nanotube arrays photocatalyst for production of hydrogen from glycerol–water solution *Int. J. Hydrogen Energy* **39** 30 16927-35
[14] Wu H and Zhang Z 2011 High photoelectrochemical water splitting performance on nitrogen doped double-wall TiO2 nanotube array electrodes *Int. J. Hydrogen Energy* **36** 21 13481-7
[15] Aritonang A B, Surahman H, Krisnandi Y K and Gunlazuardi J 2017 Photo-electro-catalytic performance of highly ordered nitrogen doped TiO2 nanotubes array photoanode *IOP Conf. Ser. Mater. Sci. Eng.* **172** 1 012005
[16] Luo N, Jiang Z, Shi H, Cao F, Xiao T and Edwards P P 2009 Photo-catalytic conversion of oxygenated hydrocarbons to hydrogen over heteroatom-doped TiO2 catalysts *Int. J. Hydrogen Energy* **34** 1 125-9
[17] Subramanian A and Wang H-W 2012 Effects of boron doping in TiO2 nanotubes and the performance of dye-sensitized solar cells *Appl. Surf. Sci.* **258** 17 6479-84
[18] Sreekantan S, Lockman Z, Hazan R, Tasbihi M, Tong L K and Mohamed A R 2009 Influence of electrolyte pH on TiO2 nanotube formation by Ti anodization *J. Alloys Compd.* **485** 1-2 478-83
[19] Lai Y-K, Huang J-Y, Zhang H-F, Subramaniam V-P, Tang Y-X, Gong D-G, Sundar L, Sun L, Chen Z and Lin C-J 2010 Nitrogen-doped TiO2 nanotube array films with enhanced photocatalytic activity under various light sources *J. Hazard. Mater.* **184** 1-3 855-63
[20] Chen Y, Zhang S, Yu Y, Wu H, Wang S, Zhu B, Huang W and Wu S 2008 Synthesis, characterization, and photocatalytic activity of N-doped TiO2 nanotubes *J. Dispers. Sci. Technol.* **29** 2 245-9